Available online at www.sciencedirect.com
ScienceDirect
Journal of the European Ceramic Society 30 (2010) 1641–1648
www.elsevier.com/locate/jeurceramsoc

Silica fume as porogent agent in geo-materials at low temperature

E. Prud'homme [a], P. Michaud [a], E. Joussein [b], C. Peyratout [a], A. Smith [a], S. Arrii-Clacens [c], J.M. Clacens [c], S. Rossignol [a,*]

[a] *Groupe d'Etude des Matériaux Hétérogènes (GEMH-ENSCI) Ecole Nationale Supérieure de Céramique Industrielle, 47-73 Avenue Albert Thomas, 87065 Limoges, France*
[b] *GRESE, EA 3040, 123 Avenue Albert Thomas, 87060 Limoges, France*
[c] *Laboratoire de Catalyse en Chimie Organique (LACCO), Université de Poitiers, UMR CNRS 6503, 40 Avenue du Recteur Pineau, 86022 Poitiers Cedex, France*

Received 14 July 2009; received in revised form 22 December 2009; accepted 10 January 2010
Available online 1 February 2010

Abstract

The synthesis of geopolymers based on alkaline polysialate was achieved at low temperature (~25–80 °C) by the alkaline activation of raw minerals and silica fume. The materials were prepared from a solution containing dehydroxylated kaolinite and alkaline hydroxide pellets dissolved in potassium silicate. Then the mixture was transferred to a polyethylene mold sealed with a top and placed in an oven at 70 °C for 24 h. For all geopolymer materials, following dissolution of the raw materials, a polycondensation reaction was used to form the amorphous solid, which was studied by FTIR-ATR spectroscopy. The in situ inorganic foam based on silica fume was synthesized from the in situ gaseous production of dihydrogen due to oxidation of free silicon (content in the silica fume) by water in alkaline medium, which was confirmed via TGA-MS experiments. This foam has potential as an insulating material for applications in building materials since the thermal measurement has a value of 0.22 W m^{-1} K^{-1}.

Keywords: Spectroscopy; X-ray methods; Thermal properties; Insulators; Silicate; Chemical properties

1. Introduction

Geopolymers are amorphous three-dimensional alumino-silicate binder materials, which were first introduced to the inorganic cementitious world by Davidovits in 1978.[1] Geopolymers may be synthesized at or slightly above room temperature by alkaline activation of alumino-silicates obtained from industrial wastes, calcined clays, natural minerals or mixtures of two or more of these materials. In a strong alkaline solution, alumino-silicate reactive materials are rapidly dissolved into solution to form free SiO_4 and AlO_4 tetrahedral units.[2,3] During the polycondensation reaction, the tetrahedral units are linked in an alternate manner to yield amorphous geopolymers. Geopolymer concretes are based on compounds that are generally produced from one or more solid components (binders) and one or more liquid components (activators), which react together to form strong, durable materials. Some binders, like PVA fibers or fly ash, have been used in technical extrusion, but not in large-scale batch preparation like concrete.[4] Furthermore, little work has been devoted to the feasibility of making geopolymer-synthesized foam without organic additives.[5–7] Among the ceramic foams, some were synthesized by the addition of H_2O_2 and aluminum powders for mechanical property applications.[8] Aluminum was also utilized in the production of lightweight refractory based on raw minerals.[9] In the same way, glass foams displaying efficient compressive strength were obtained using sheet-glass cullet with dolomite or calcite as the foaming agent.[10]

Among the different families of geopolymers, those based on potassium rather than sodium present modified thermal and mechanical properties due to the larger size of the potassium ion.[11–13]

Currently, there is a political as well as a societal demand for products that require less energy for the manufacturing process and are easy to recycle. The new materials have to display properties comparable to or better than those of existing materials.

* Corresponding author. Tel.: +33 5 55 45 22 24.
E-mail address: sylvie.rossignol@unilim.fr (S. Rossignol).

0955-2219/$ – see front matter © 2010 Elsevier Ltd. All rights reserved.
doi:10.1016/j.jeurceramsoc.2010.01.014

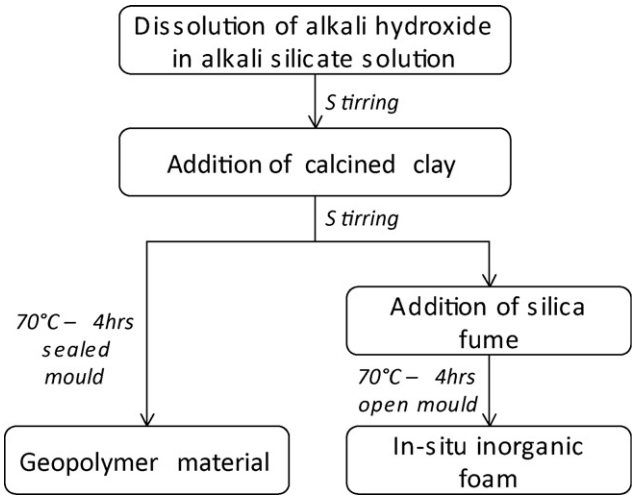

Fig. 1. Synthesis protocol of geo-materials and in situ inorganic foam.

Traditional materials associating mineral binders and local raw materials can be found in all cultures and time periods.[14] However, the physical chemistry of the exchanges between the various components of the composite is not well known. Furthermore, new cementitious materials known as geopolymers, including generally silicates or alumino-silicates, can be used as substitutes for conventional hydraulic binders.[15] However, the control of consolidation time, hydraulic behavior and the subsequent working properties of the materials remain difficult. Geopolymer materials could also be used to passivate industrial waste and as an alternative to cements.

The aim of this work was to determine the composition of a geopolymer based on potassium polysialate from raw minerals. The incorporation of silica fume was also studied to the in situ production of a geopolymer-foam based on potassium silicate. The understanding of the polycondensation reaction of the various samples was determined by in situ ATR, XRD and by thermal analysis coupled with mass spectrometry.

2. Experimental part

2.1. Samples preparations

The initial geo-material was prepared from a solution containing dehydroxylated kaolinite and KOH pellets (85.7% of purity) dissolved in potassium silicate (Si/K = 1.66, density 1.33), as described in Fig. 1. The reactive mixture was then placed in a sealed polystyrene mold in an oven at 70 °C for 4 h to complete the polycondensation reaction. Then the material was removed from the mold and placed in an oven at 70 °C for 24 h for drying. To improve the thermal properties for industrial waste, silica fume supplied by FEROPEM (France) was added to the reaction mixture and placed in an oven at 70 °C in an open mold. This additive displays an amorphous character with a nanometer size. Its particularity is the presence of a small amount of free silicon (Table 1). Different geo-materials with varying molar ratios (nSi/nK; nSi/nAl) were synthesized (Table 2).

Table 1
Composition of various samples.

Ratio	n_{Al}/n_{Si}	n_K/n_{Al}	n_K/n_{Si}
Geopolymer	0.64	0.78	0.50
F_i	0.27	1.51	0.41
F 0Si	0.48	1.51	0.73
F 2Si	0.45	1.51	0.67
F 5Si	0.40	1.51	0.61
F 10Si	0.34	1.51	0.52
F 14Si	0.30	1.51	0.46
F 21Si	0.24	1.51	0.37
F 0KOH	0.27	0.65	0.17
F 1KOH	0.27	0.73	0.20
F 3KOH	0.27	0.86	0.23
F 5KOH	0.27	1.08	0.29
F 8KOH	0.27	1.30	0.35
F 13KOH	0.27	1.73	0.46

2.2. Characterization

FTIR spectra were obtained from a ThermoFischer Scientific 380 infrared spectrometer (Nicolet) using the attenuated total reflection (ATR) method. A drop of geopolymer reacting mixture was deposed on the diamond crystal and protected by a little bell from environmental pollution during the spectrum acquisition, which was performed regularly until the end of geopolymerisation. The IR spectra were gathered between 500 and 4000 cm^{-1} with a resolution of 4 cm^{-1}. OMNIC (Nicolet Instruments), the commercial software, was used for data acquisition and spectral analysis.

X-ray patterns were acquired via X-ray diffraction (XRD) experiments on a Brucker-AXS D 5005 powder diffractometer using Cu Kα radiation ($\lambda_{K\alpha}$ = 0.154186 nm) and a graphite back-monochromator. XRD patterns were obtained using the following conditions: dwell time: 2 s; step: 0.04°. Crystalline phases were identified by comparison with PDF standards (Powder Diffraction Files) from ICDD. In situ X-ray measurements were carried out in a high temperature stainless steel chamber HTK16 linked to a Brucker-AXS D8 Advance diffractometer. The diffractograms were recorded in steps of 0.028° with a dwell time of 10 s. The powdered oxides (about 20 mg) were suspended in ethanol and deposited as a thin layer on a Kanthal foil supporting the sample and heated via the Joule effect. The sample was heated in air from 25 to 1000 °C at a heating rate of 0.10 °C s^{-1}.

Table 2
Main vibration bands of Si–O species[19,21].

Wavenumber (cm^{-1})	Type	Bond
798 (m)	Symmetric stretching	Si–O–Si
727	Symmetric stretching	Si–O–Si
1115–1140	Asymmetric stretching	Si–O–Si
1165 (sh)	Asymmetric stretching	Si–O–Si
1080	Asymmetric stretching	Si–O–Si
466	Bending	Si–O–Si
560	Symmetric stretching	Al–O–Si
1077	Asymmetric stretching	Al–O–Si
840	Rocking	Si–OH

The morphology of the final products was determined using a Cambridge Stereoscan S260 scanning electron microscope (SEM). Prior to their observation, a carbon layer was deposited on the samples. The average pore size was calculated using the Image J program based on a counted number of 500.

Differential thermal analysis (DTA) and thermogravimetric analysis (TGA) were performed to characterize the solids. TDA–TGA experiments were carried out in a Pt crucible between 25 and 1200 °C using a Setaram Setsys evolution. The samples were heated at 10 °C min^{-1} in dry airflow.

Thermogravimetric analysis coupled with mass spectrometry (TGA-MS) was performed on a SDT Q600 apparatus from TA Instruments coupled by a heated capillary column with a Prisma QMS 200 mass spectrometer from Balzers. To measure the amount of H_2 formed, the samples were heated to 70 °C (heating rate: 5 °C/min) and maintained at this temperature for 2 h under a dry air flow (100 mL/min). The fresh foam thermal analysis was performed up to 800 °C (heating rate: 5 °C/min) under Ar (100 mL/min).

Thermal properties were determined using the "Laser Flash" method as described by the work of Michot et al.[16] Cylindrical samples were synthesized with a thickness of approximately 2 mm.

3. Results

3.1. Formulation of geo-material

A material with the formulation $K^+_{0.10}[(SiO_2)_{1.63}AlO_2]_{0.10}$, $0.67H_2O$ was first synthesized from dehydrated kaolinite obtained from calcined (700 °C) kaolin supplied by IMERYS France. The formation of this geo-material was the result of a geopolymerization reaction involving the restructuration of material. This phenomenon was followed by ATR spectroscopy. A drop of reactant mixture was put on the diamond crystal protected by a cover, which prevented the water evaporation from the mixture at room temperature. These conditions were necessary to promote polycondensation in the closed environment.[17] The spectra shown in Fig. 2 were recorded as a function of time.

The bands on the spectra at $t = 0$ h, at 3255 and 1620 cm^{-1}, were attributed to Si–O–H bond and to water, respectively. Their intensity gradually diminished with time.[18] The bands due to Si–O–M bonds [19,20] (M = Si, Al, K) were located in the 1100–950 cm^{-1} range and their precise positions depended on the length and bending of the Si–O–M bond as presented in Table 2. The decrease of the OH bands compared to the Si–O–Al bands was due to the increase in the polycondensation time and was characteristic of the formation of geo-material. Furthermore, the Si–O–M$^+$ [21] shift from 979 to 946 cm^{-1}, also in agreement with the literature data, gives evidence for dissolution of the metakaolin species by the basic environment.[22] This experiment as a function of time proved that a reaction time of 17 h was sufficient to achieve a consolidated geo-material at room temperature.

The resulting XRD pattern (Fig. 3) displayed a broad peak characteristic of an amorphous material. The calcination at 700 °C of kaolin involved the transformation in dehydrated kaolinite, but some crystallized peaks were also detected were due to traces of illite or feldspar clays present as contaminants, which were not eradicated at this temperature. The shift in 2θ peak position observed in the geo-material XRD pattern by comparison with the dehydroxylated kaolinite XRD pattern provides evidence for dissolution of SiO_4 and AlO_4 species, coming from dehydrated kaolinite, into the alkaline environment during the geopolymerization reaction, as detected by ATR measurements.

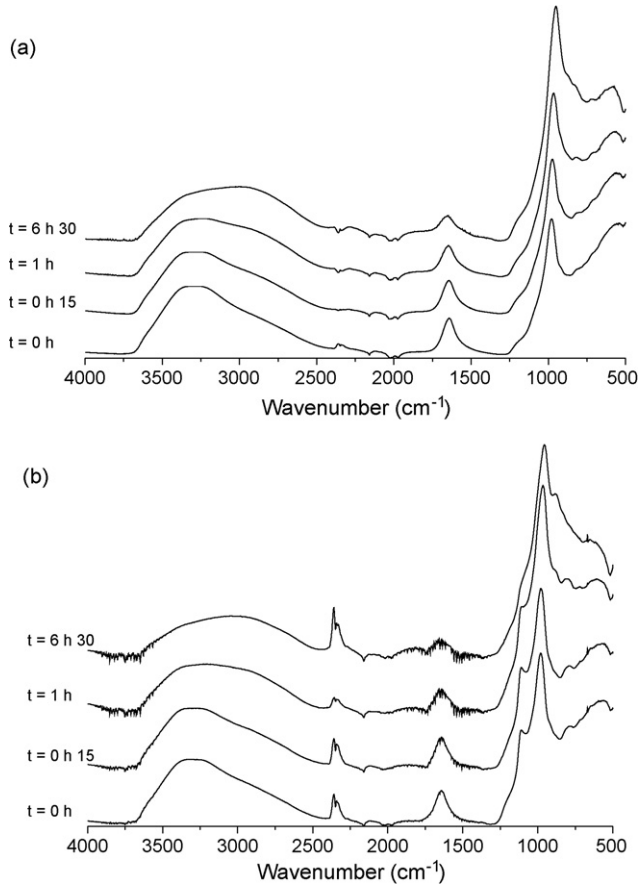

Fig. 2. In situ infrared spectra of (a) the geopolymer and (b) in situ mineral foam at 20 °C as a function of the polycondensation time.

The temperature-dependent behavior was studied via thermal analysis (Fig. 4). The endothermic peak below 400 °C associated with a weight loss was attributed to free water and hydroxyl condensation. The weight loss of ~12% is in agreement with the work of Duxson et al.[23] Above this temperature, the geo-material was stable with temperature up to 800 °C.

3.2. Addition of silica fumes

3.2.1. Potassium foam

To increase the thermal resistance by creating porosity in the geo-material, the addition of silica fumes has been investigated. The addition of silica fume to a solution containing SiO_2, K_2O, Al_2O_3 and KOH issue from the various base raw materials (metakaolin, potassium silicate and potassium hydroxide) gave a very reactive mixture that resulted in the formation of in situ inorganic foam. This new compound can be considered a geo-material since the XRD pattern is characteristic of

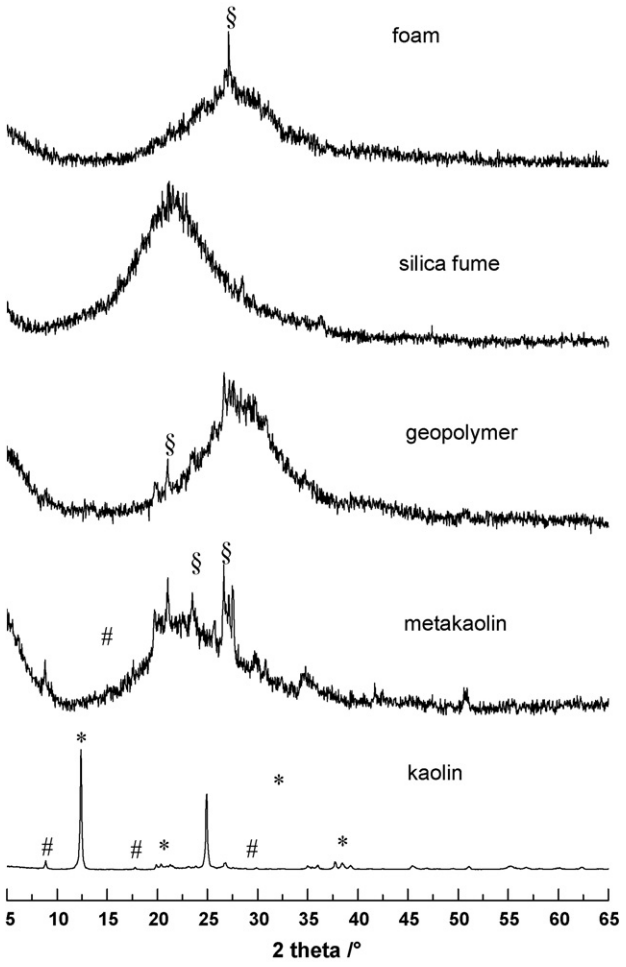

Fig. 3. XRD patterns of kaolin, metakaolin, geopolymer, silica fume and foam. (PDF files *: kaolinite (01-089-6538); #: illite (00-002-0056); §: Sanidine (04-009-6667)).

an amorphous material (Fig. 3). Effectively, the maximum of diffracted intensity is positioned at similar 2θ values for both the original geo-material and the inorganic foam. Moreover, since the XRD peaks of the silica fume disappear in the foam XRD pattern, the formation of this compound involves the dissolution or transformation of the small local order of silica fume. Another process could also take place, as indicated by the presence of the diffraction peak attributed to the feldspar ($KAlSi_3O_8$) compound.

To find evidence of disorder in the silica fume lattice, the synthesis of inorganic foam was studied by ATR spectroscopy (Fig. 2). The main bands detected for the geo-material were observed on the various foam spectra and in fact the decrease of the OH and Si–O–M bands was faster in the geo-material. The polycondensation reaction in the foam seemed to be finished after 4 h 30 min compared to 17 h for the geo-material. However, new bands also appeared and were located at 1110, 914, 880, 800 and 670 cm^{-1}, corresponding respectively to Si–O–T,[22] Al–OH, Si–O–Si,[24] Si–O–Al,[21] and O–Si–O.[19] The decrease of the band at 1110 cm^{-1} linked to amorphous silica confirmed the loss of short-range order of the silica fume always seen in the XRD pattern. At the same time, the band at 880 cm^{-1} due to stretching vibration of Si–OH increased, revealing the consummation of water involving non-bridging oxygen atoms. Similarly, the bands located at 914 and 800 cm^{-1} showed the attack of the Al–O species during geopolymerization, which was not clearly observed for the geo-material. Another band at 670 cm^{-1} could be attributed to a zeolite species.[25] These experiments proved the almost-complete dissolution of raw materials to create the in situ inorganic foam.

3.2.2. *Effect of silica fume addition*

To understand the inorganic foam formation as a function of the amount of each reactant, experiments based on constant KOH or silica fume amounts were performed (Fig. 5(a) and (b)). The F_i sample was characteristic of the first in situ foam synthesized (Table 2). The ratio of the final initial volume was given to compare the influence of both components depending on the molar ratio. The increase of the final volume in relation to the amount of silica fume (Fig. 5(a)) revealed the important role of this compound for in situ inorganic foam formation. Nevertheless, the amount of silica fume must be at least 50 wt.% to get a significantly porous material. For higher values, the volume enhancement was proportional to the silica amount and corresponded to an initial ratio of $n_{Si}/n_K \approx 2.5$. The amount of KOH (Fig. 5(b)) must be at least 10 wt.% to involve a notable volume expansion. The composition of this sample was close to $n_{Al}/n_K \approx 1$ and $n_{Si}/n_K \approx 3.5$. These ratio values are close

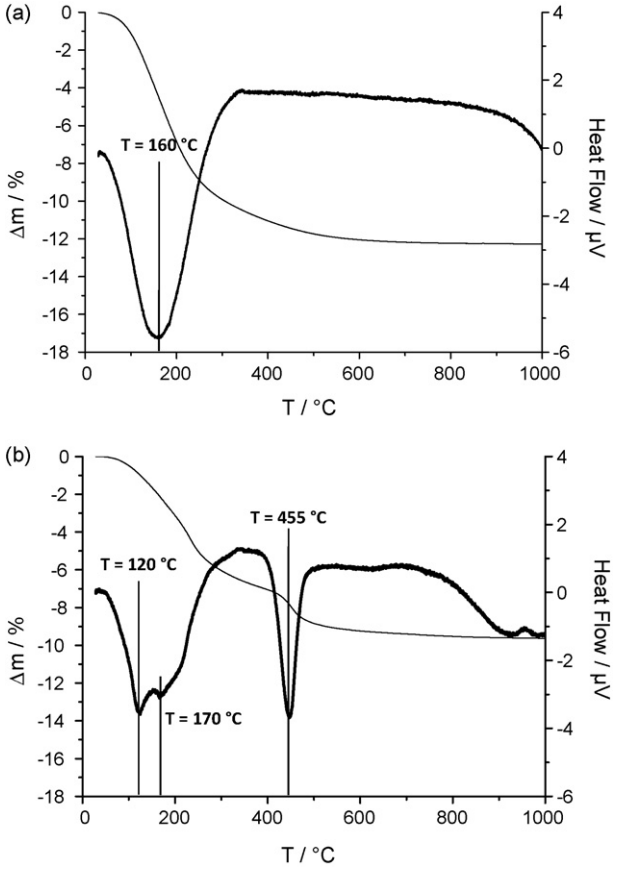

Fig. 4. Thermal analysis of the (a) geopolymer and (b) foam.

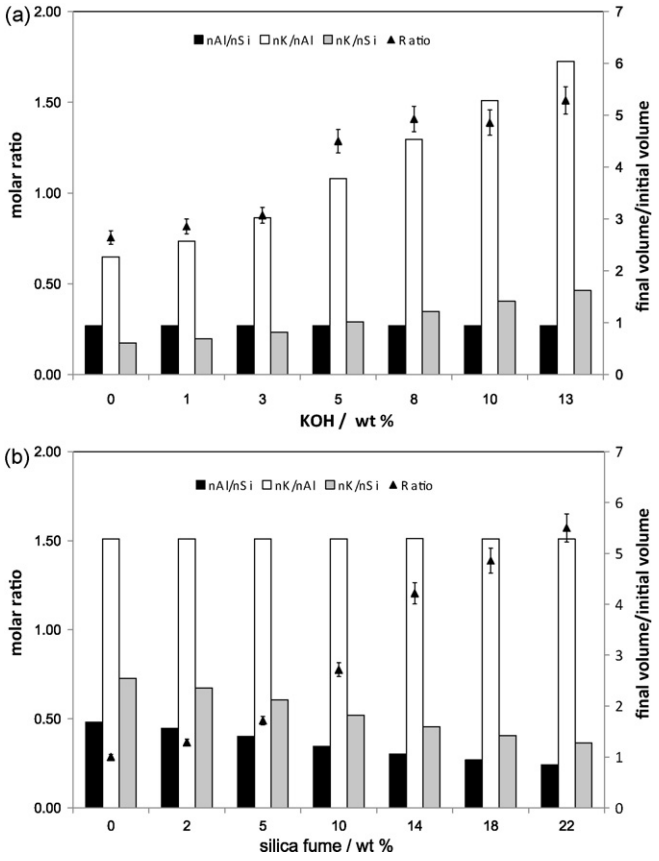

Fig. 5. Ratio (▲) of the final volume vs. the initial volume of each sample after a curing at (70 °C, 6 h) as a function of the various Si, Al and K ratios for (a) KOH and (b) silica fume constant amounts.

to those found in the feldspar compound identified by XRD measurement, which must be investigated.

3.2.3. Control of porosity

To understand how porosity might be controlled, investigations were performed during sample drying at 70 °C for a period of 7 days. Only three experiments are shown in Fig. 6, representing the removal of the sample from the mold after □ 6 h, ■ 2 days and ■ 7 days. The comparison of the pore sizes depends strongly on the time before mold removal. Without removal, the obtained foam displayed a large range of sizes with an average pore size of approximately 0.37 mm. Removal after 48 h involved a slight decrease in size, but the heterogeneous scale was displaced to the small pores. The smallest pore size displaying a diameter of 0.13 mm was achieved by removal of the mold after 6 h. This foam was characterized by some ladder like structure with 0.02 μm diameter windows. We could deduce that these drying conditions can be applied to some extent to control the pore size. The microstructure of the synthesized foam could be compared to that of other metal foams.[26] The range in porosity due to the removal at different times can also be explained by the production of a gas involving coalescence in a part of the foam, such as the center, as noted by Jim et al.[27]

3.2.4. Behavior with temperature

To more precisely understand the behavior of the foam under high thermal treatment, thermal analysis was performed and the results are reported in Fig. 4b. The two endothermic peaks at 170 and 455 °C could be correlated with two weight losses that led finally to a value close to that of the geo-material. To understand

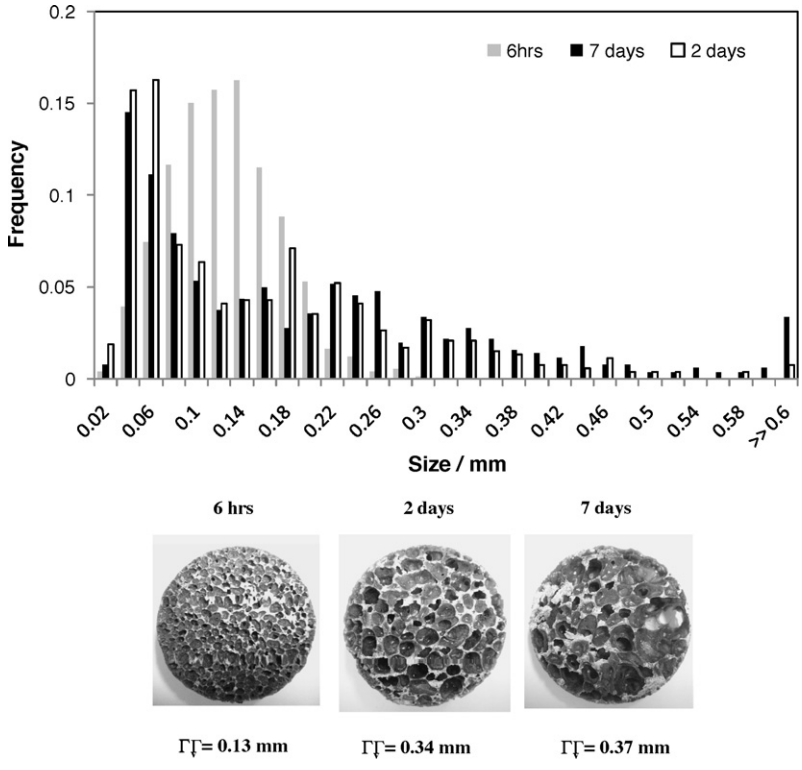

Fig. 6. See other file.

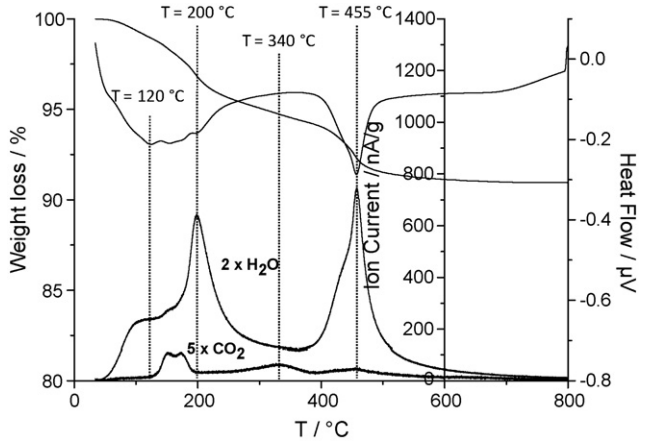

Fig. 7. Thermal analysis coupled with mass spectrometry of fresh foam.

the endothermic peaks, an experiment based on thermal analysis coupled with a mass spectrometer was performed on the foam and the results are reported in Fig. 7. The first endothermic peak at 120 °C simultaneous with water outgassing matches to the loss of free water, the second peak at 170 °C to gaseous CO_2 from some carbonated species that occurred on the surface or from a carbonate species formed during the synthesis by some C element as impurities issued from the silica fume. The detection of CO_2 gas at 340 °C may be due to the decomposition of a potassium hydrogenous compound or potassium carbonate compound. The determination of these species was very difficult due to their low quantities. The last endothermic peak at 455 °C is essentially due to the loss of structural water. The carbonate species can be explained by some potassium element which can form hydrogenous or carbonate potassium ($KHCO_3$ or K_2CO_3) during aging between the synthesis and the experiments. To understand the weight loss that occurs at around 400 °C, we performed the in situ XRD measurements given in Fig. 8. The XRD pattern at room temperature was characteristic

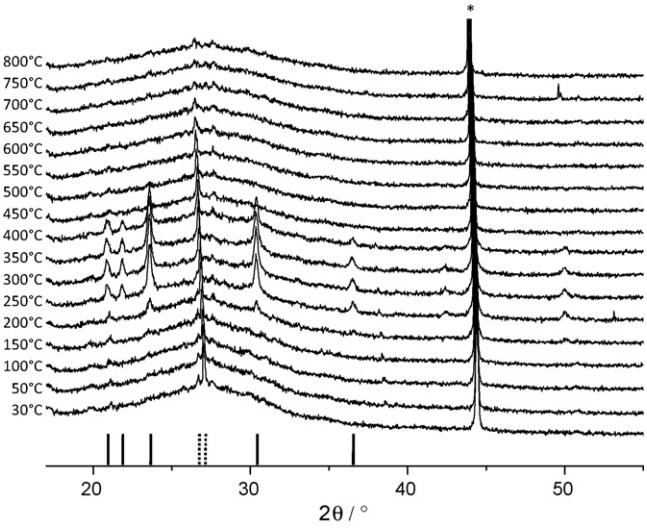

Fig. 8. In situ XRD patterns of potassium foam as a function of temperature under air (PDF files: — $KAl_4Si_2O_9(OH)_3$ 01-070-3754; ..... $KAlSi_3O_8$ 00-025-0618; *: Kanthal support).

of a mixture of amorphous compounds and to peaks attributed to SiO_2 (quartz) and to $KAlSi_3O_8$ feldspar. During heating, a phase that could be ascribed to hydrated potassium aluminum silicate (type $KAl_4Si_2O_9(OH)_3$) appeared at around 200 °C (Fig. 8). Its decomposition leads to the loss of water observed on the TGA curve by the endothermic peak at about 450 °C and to this disappearance at 450 °C from the XRD pattern, implying that it would be a metastable phase. The phenomenon responsible of this structural change could be due to the diffusion of some species associated simultaneously with the loss of CO_2 issued from hydrogenous or carbonate species. These species are also identified by some experiments based on the durability of samples. In fact, these samples are stable in basic and neutral medium whereas they are cleaned in acidic medium due to the carbonate species linked to the potassium element which could migrate.[28]

3.2.5. An explanation for the porosity

An explanation of inorganic in situ foam formation can be proposed based on (i) the production of a gas, (ii) an increase of the viscosity and (iii) a consolidation of material. The generation of porosity was probably due to the H_2 produced by water reduction (Eq. (1)) and by the oxidation of silicon in an basic environment (Eq. (2)), ensuring to the formation of $Si(OH)_4$ species (Eq. (3)).

$$Si^0 \rightarrow Si^{4+} + 4e^- \quad (1)$$

$$4H_2O + 4e^- \rightarrow 2H_2 + 4OH^- \quad (2)$$

$$4H_2O + Si^0 \rightarrow 2H_2 + Si(OH)_4 \quad (3)$$

The dihydrogen production behaved as a foaming agent. In fact, during this redox reaction, the addition of silica fume simultaneously induces the dissolution of silica in a basic medium and the formation of $Si(OH)_4$ neutral species detected by the presence of the Si–OH band after 15 min (Fig. 2B). This phenomenon can also be observed in the XRD pattern (Fig. 3B) in the form of a 2-theta shift, revealing a small local order transformation in the silica. Consequently, the mixture diminishes in charged species, making it possible to create a reversible physical gel that will have a high silica concentration. As the reaction progresses, the Si–O–Al species dissolves and water is produced. This results in dilution of the charged silica solution, giving a specific value, and the solution turns into a chemically irreversible gel. From this value, the formation of a locally built network gel comprised of the aluminum potassium silicium oxide compound may occur. Consequently, the increase in viscosity with the high density of silica particles[27] arises from the lattice gel becoming increasingly rigid where the diffusion of the gas is enhanced. As such, the porosity was probably generated as a result of both the gel formation and the increase of viscosity in relation with the temperature increase as observed during the drying step.

An experiment-based thermal analysis coupled with mass spectrometry of the geopolymer and the foam is given in Fig. 9. The experimental conditions corresponded to the reactant mixture put in the apparatus at 70 °C under dried air. The current ion intensities were corrected by the mass of the introduced sample. Only the mass corresponding to water ($m/e = 18$) and dihydrogen

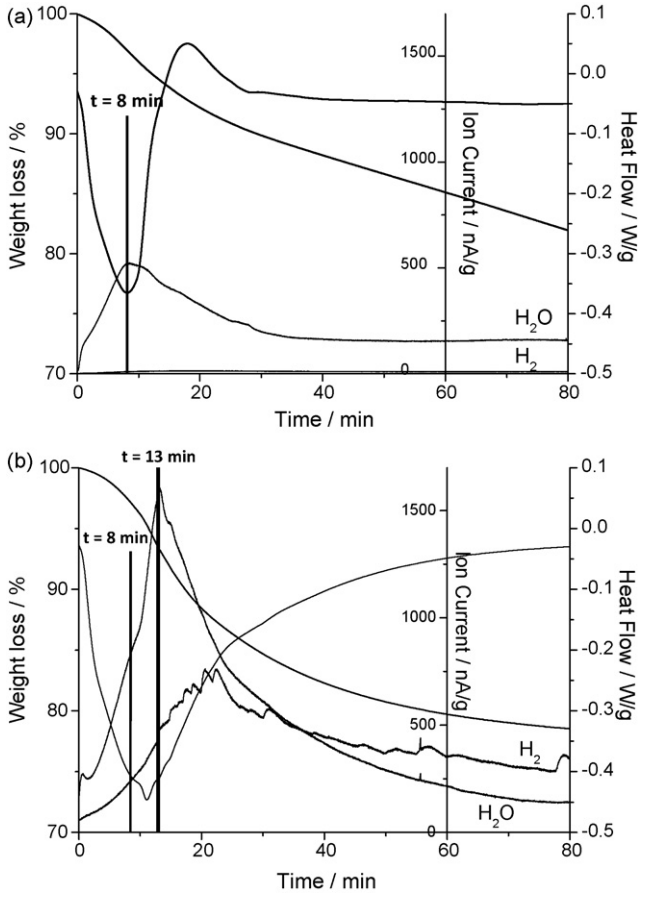

Fig. 9. Mass-spectroscopy coupled with DTA and TGA measurements during (a) geopolymer formation and (b) foam formation.

($m/e = 2$) were significant. Whatever the sample, an endothermic peak was observed and its intensity was a function of the nature of the sample. For the geopolymer, the endothermic peak was very small and short, and no variation was detected after 20 min. For the foam, this endothermic peak was very significant and large. These first results suggest that the foam formation requires the production of water, producing an endothermic thermal flux observed in both the curves. It seems that the kinetic reaction of the production of water depends on the sample, since the production of water as a result of current ion was in perfect correlation with the endothermic peak. The intensity of this peak is determined by the combination of at least two phenomena including (i) the reaction of silanol condensation (2Si–OH = Si–O–Si), leading to water, and (ii) the water production due to the exothermicity of the reaction involving cold and heat transfer during the reaction. The water amount deduced from MS curves being less pronounced in the case of the geopolymer than for the foam could be explained by the exothermicity of the reaction due to the production of gas. The endothermic peak (foam sample) can be explained by the contribution of two types of water. The first appears identical to that observed on geopolymer sample and the second can be linked to the production of H_2. In fact, the production of H_2 consumes a weak amount of water (1.1% molar) present on the medium. The difference of intensity (Fig. 9(a) and (b)) could be the result of

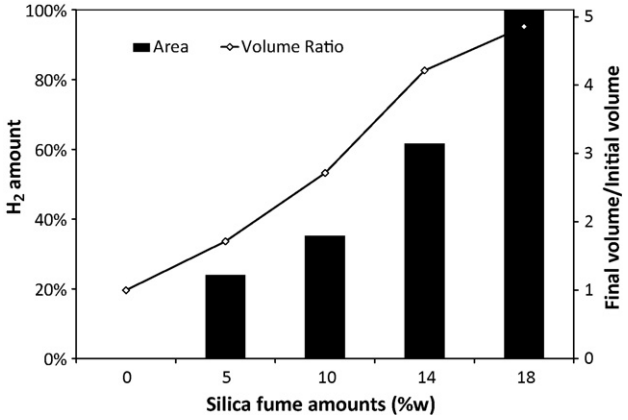

Fig. 10. Ratio of final volume vs. initial volume obtained from each sample after a curing at (70 °C, 6 h) and the dihydrogen amount deduced from DTA-SM experiments at 70 °C as a function of the silica fume amount.

a weak consolidation in the case of foam in relation to geopolymer sample. In the case of a weak or slow down consolidation due to a change in viscosity, the water loss can be or not promoted. The major difference on the MS curves between the two samples resides in the peak resulting from the dihydrogen on the foam sample, which evidences the formation of gas bubbles, which promote the construction of foam. In addition, this formation was accomplished simultaneously by a slow decrease of the water content as mentioned above. In fact, the weak amount of Si^0 (0.3%) issuing from the silica fume was sufficient, according to Eq. (3), to produce a gas responsible for the increase in the final volume compared to the initial volume, consuming only 1% of the water present in the medium. To check this theory, we have reported in Fig. 10 the amount of dihydrogen calculated from DTA-MS measurements and the final volume vs. initial volume as a function of the weight-percentage of silica fume introduced in the mixture during the synthesis for various samples. The dihydrogen-outgassing of the F_i sample was taken as a reference for the percentage calculated. The amount of dihydrogen increasing linearly as the final volume vs. initial volume ratio corroborated the role played by the silica fume producing dihydrogen.

In summary, the formation of this foam was based on the production of dihydrogen responsible for the final volume vs. the initial volume, which played a major role in the increase of the viscosity, leading to the consolidation of the material.

3.3. Thermal properties

The thermal diffusivity was determined by via "laserflash" method, with a value of $5.9 \times 10^{-7}\,m^2\,s^{-1}$. The amorphous character of this foam implied that the nature of the bond in the sample was relatively complex, and did not allow for the establishment of an exact value of the heat capacity. Nevertheless, the major constituents permitted estimation of the value to be between 700 and $1000\,J\,kg^{-1}\,K^{-1}$. From the density of $534\,kg\,m^{-3}$, a value for the thermal conductivity between 0.22 and $0.24\,W\,m^{-1}\,K^{-1}$ can be calculated, classifying this material as a good insulator material.

4. Conclusion

Geopolymers are materials with interesting chemical and physical properties in relation to their preparation feasibility. Their reinforcement at room temperature implies potential application to cements. We have successfully achieved the synthesis of various consolidated materials (geopolymer, in situ inorganic foam) prepared from a mixture containing potassium silicate, potassium hydroxide, dehydroxylated kaolinite and silica fume. The reaction of geopolymerization was studied by in situ ATR spectroscopy with a particular attention to the presence of a band at 950 cm^{-1} characteristic of the end of geopolymerization reaction. The amorphous nature of the samples was investigated via XRD, which revealed the dissolution of raw materials signifying the presence of SiO_4 and AlO_4 species isolated in the solid.

The addition of silica fume to this geo-material has involved modifications of the chemistry and in the porosity of the sample via the formation of dihydrogen during the synthesis. The inorganic foam was characteristic of a porous material where the size could be controlled by drying and by the chemistry, notably the molar ratio of Si/Al and Si/K. Furthermore, this in situ inorganic foam was characterized as an insulating material.

References

1. Davidovits J. *Chemistry and applications*. USA: Institut Géopolymère; 2008.
2. H. Xu, Geopolymerisation of aluminosilicate minerals, *PhD thesis*, Department of Chemical Engineering, University of Melbourne, Australia; 2001.
3. Grutzeck MW, Siemer DD. Zeolites synthesised from class F fly ash and sodium aluminate slurry. *J Am Ceram Soc* 1997;**80**(9):2449–58.
4. Li Z, Zhang Y, Zhou X. Short fiber reinforced geopolymer composites manufactured by extrusion. *J Mater Civil Eng* 2005;**17**(6):624–31.
5. Wu JP, Boccaccini AR, Lee PD, Rawlings RD, Thermal. Mechanical properties of a foamed glass ceramic material produced from silicate waste. *Eur J Glass Sci Technol A* 2007;**48**(3):133–41.
6. Barbosa V, Mackensie K. Synthesis and thermal behaviour of potassium sialate. *Mater Lett* 2003;**57**:1477–82.
7. Fletcher RA, MacKenzie KJD, Nicholson CL, Shimada S. The composition range of aluminosilicate geopolymers. *J Eur Ceram Soc* 2005;**25**:1471–7.
8. Bell JL, Kriven WM. Preparation of ceramic foams from metakaolin-based geopolymer gels. *Ceram Eng Sci Proc* 2009;**29**(10):97–112.
9. Jettner T, Moertel H, Svinka V, Svinka R. Structure of kaoline-alumina based foam for high temperature applications. *J Eur Ceram Soc* 2007;**27**:1435–41.
10. Fernandes HR, Tulyaganov DU, Ferreira JMF. Preparation and characterization of foams from sheet glass and fly ash using carbonates as foaming agents. *Ceram Int* 2009;**35**:229–35.
11. Duxson P, Lukey GC, Van Deventer SJ. Thermal conductivity of metakaolin geopolymers used as a first approximation for determining gel interconnectivity. *Ind Eng Chem Res* 2006;**45**:7781–8.
12. Nair BG, Zhao Q, Cooper RF. Geopolymer matrices with improved hydrothermal corrosion resistance for high temperature applications. *J Mater Sci* 2007;**42**:3083–91.
13. Phair JW, Van Deventer JSJ. Effect of the silicate activator pH on the microstructural characteristics of waste based geopolymers. *Int J Miner Process* 2002;**66**(1–4):121–43.
14. Kirshner AV, Harmuth H. Investigation of geopolymer bonders with respect to their application for building materials. *Ceramics – Silikáty* 2004;**48**:117–20.
15. Yunsheng Z, Wei S, Zongjin L, Xiangmimg Z, Chungkong C. Impact properties of geoplymer based extrudated incorporated with fly ash and PVA short fiber. *Constr Build Mater* 2008;**22**:370–83.
16. Michot A, Smith DS, Degot S, Gault C. Thermal conductivity and specific heat of kaolinite: evolution with thermal treatment. *J Eur Ceram Soc* 2008;**28**:2639–44.
17. J. Davidovits. Synthetic mineral polymer compound of the silicoaluminates family and preparation process, *US Patent, 4,472,199*;1984.
18. Innocenzi P. Infrared spectroscopy of sol–gel derived silica-based films: a spectra-microstructure overview. *J Non-Cryst Solids* 2003;**316**:309–19.
19. Criado M, Polomo A, Fernandez-Jiménez A. Alkali activation of fly ashes. Part 1. Effect of curing conditions on the carbonation of the reaction products. *Fuel* 2005;**84**:2048–54.
20. Davidovits J. Scientific tools, X-rays, FTIR, NMR. *Geopolym: Chem Appl* 2008:61–76.
21. Lee WKW, Van Deventer JSJ. Use of infrared spectroscopy to study geopolymerization of heterogeneous amorphous aluminosilicate. *Langmuir* 2003;**19**:8726–34.
22. Rees CA, Provis JL, Luckey GC, Van Deventer JSJ. Attenuated total reflectance Fourier transform infrared analysis of fly ash geopolymer gel aging. *Langmuir* 2007;**23**:8170–9.
23. Duxson P, Lukeyand GC, Van Deventer JSJ. Thermal evolution of metakaolin geopolymer. Part 1. Physical evolution. *J Non-Cryst Solids* 2006;**352**:5541–55.
24. Uchino T, Sakka T, Hotta K, Iwasaki M. Attenuated total reflectance Fourier-transform infrared spectra of a hydrated sodium silicate glass. *J Am Ceram Soc* 1989;**72**(11):2173–5.
25. Breck DW. *Zeolite molecular sieves: structure, chemistry and use*. New York: Wiley-Interscience; 1974. p. 415–418.
26. Binner J, Chang H, Higginson R. Processing of ceramic metal interpenetrating composites. *J Eur Ceram Soc* 2009;**29**:837–42.
27. Jim H, Lee S, Han Y, Park J. Control of pore size in ceramic foams: influence of surfactant concentration. *Mater Chem Phys* 2009;**113**:441–4.
28. Prud'homme E. , Michaud P., Joussein E., Peyratout C., Smith A., Rossignol S.; in preparation.